erosion of softer rocks form linear gullies allowing the river to flow through them.

We argue that the current flow path of River Narmada, between Bhedaghat and Saraswati Ghat is largely guided by the gorges formed due to erosion of Proterozoic dykes. The origin of the Dhuadhar Falls, is therefore, related to the preferential weathering of talcose material, which is the metamorphosed product of mafic Proterozoic dykes over the hard weathering-resistant marbles and schists. We summarize the hypothesis as follows: The Narmada once flowing gently in this region along its palaeo channel, guided by the basement rooted NSL, changes its path and falls into the deep gorges formed by weathering and erosion of metamorphosed dykes and forms the Dhuadhar Falls at its current location (Figure 2 *e*).

1. Ahmed, F., *Curr. Sci.*, 1964, **33**(12), 362–363.
2. Kale, V. S., Doctoral dissertation, Poona University, Pune, 1985.
3. Naqvi, S. M. and Rogers, J. W., *Geol. J.*, 1987, **23**, 281–345.
4. Kumar, M. R., Singh, A., Kumar, N. and Sarkar, D., *Precambrian Res.*, 2015, **270**, 155–164.
5. Mall, D. M., Singh, A. P. and Sarkar, D., *Curr. Sci*., 2005, **88**(10), 1621–1266.
6. Murty, T. V. V. G. R. K. and Mishra, S. K., *J. Geol. Soc. India*, 1981, **22**, 112–120.
7. Qureshy, M. N., *Photogrammetria*, 1982, **37**, 161–184
8. Mahmood, R., Babel, M. S. and Jia, S., *Weather Climate Extremes*, 2015, **10**, 40–55.
9. Pan, S., *Int. J. Geomat. Geosci.*, 2013, **4**(1), 149–163.

Received 16 April 2018; accepted 26 February 2019

JYOTIRMOY MALLIK*
AYANANGSHU DAS
SHREEJA DAS
KRISHANU BANDYOPADHYAY

Earth and Environmental Sciences,
Indian Institute of Science Education and Research,
Bhopal Bypass Road, Bhauri,
Bhopal 462 066, India
**For correspondence.*
e-mail: jmallik@iiserb.ac.in

Uranium mineralization in Kappatralla outlier of Gulcheru quartzite formation, Mesoproterozoic Cuddapah Supergroup, Kurnool district, Andhra Pradesh, India

In the eastern Dharwar craton, the crescent-shaped Cuddapah Basin forms a large intracratonic basin, comprising Meso–Neoproterozoic sedimentary sequence with volcanic rock components. The sedimentary environment of the Cuddapah Basin, in general, is comparable with peri-tidal complex with shallow marine carbonate shelf and beach environment. Systematic geological studies of the Cuddapah Basin are well documented[1,2]. The litho-units of the basin are mainly divided into older Cuddapah Supergroup and a younger Kurnool Group. The former is present throughout the basin, while the younger group is seen in its western and northeastern parts. The sediments of the basin overlie the Late Archaean–Lower Proterozoic granitoids intruded by basic and ultrapotassic dykes.

Investigations by the Atomic Minerals Directorate for Exploration and Research (AMD) resulted in identifying syngenetic strata-bound uranium mineralization at Tummalapalle, Andhra Pradesh (AP) and epigenetic unconformity proximal as well as fracture-controlled uranium deposits in Lambapur, Chitrial and Peddagattu areas of Telangana, India. The unconformity contact between the basement granites and overlying sediments of Cuddapah/Kurnool Groups is one of the potential targets for unconformity-type uranium mineralization along the northern and western margins of the arcuate Cuddapah Basin. Uranium mineralization has also been recorded in siltstone and quartzite of Gulcheru Formation associated with E–W fault near Gandi[3] and Tipparajupalle and Cheruvula Bodu areas of Cuddapah district[4] along the southern margin of Cuddapah Basin.

Here we focus on uranium mineralization in the outlier of the Gulcheru Formation near Kappatralla, Kurnool district, AP.

The Geological Survey of India[5] reported an isolated outlier of Gulcheru quartzite with an aerial extent of about 3.5 km^2 near Kappatralla village (15°34′35″N; 77°36′19″E, Survey of India toposheet no. 57 E/10), which is situated about 35 km west of Veldurthi, Kurnool district, India.

In the Kappatralla outlier, the Gulcheru quartzite rests as a cover rock above the basement crystalline rocks. The basement is composed of granite gneiss, granodiorite, diorite and intrusive granite equivalent of Closepet Granite. The intrusive granites are medium- to coarse-grained, grey biotite granite with several pegmatite and aplite veins intruded by NW–SE and E–W trending dolerite dykes (Figure 1). The NW–SE trending fractures in the granitoids are filled by chlorite, hematite and sericite due to hydrothermal alteration along fractures.

The unconformity contact between the basement granites and overlying Gulcheru quartzite approximately follows 540 m RL contour and the highest elevation of the outlier is 567 m. The thickness of Gulcheru sediment thus varies from 10 to 25 m. The Formation commences with lower pebbly feldspathic quartzite at the base which is successively overlain by ferruginous quartzite, grey sub-feldspathic quartzite, exhibiting current bedding and ripple marks with intercalation of carbonaceous, purple and greenish-grey shale, buff-brown quartzite and pebbly quartzite at the top with pebbles of quartz. Figure 2 shows the litho-facies diagram of Gulcheru quartzite in the study area. The strike of the formation is 45°–50°N with 4°–6° dip due SE. Uraniferous sub-feldspathic Gulcheru quartzite is light grey, composed of moderately sorted quartz grains with angular feldspar grains. They also contain bands, laminae and lenses of carbonaceous

shale. The buff-brown quartzite is dissected by NW–SE and N–S trending fractures; among them the NW–SE fractures are prominent.

Kappatralla outlier exhibits a favourable set-up for unconformity-type uranium mineralization having late Archaean to early Proterozoic granites as favourable basement, and sediments and Proterozoic Gulcheru quartzite as cover rock. Systematic radiometric survey and subsurface exploration in and around the outlier revealed uranium mineralization in both the basement and cover rock. Lateral continuity of uranium mineralization in Gulcheru quartzite is indicated in the bore holes drilled thus far. The gamma-ray logging results indicated grade varying from 0.013% to 0.19% eU_3O_8, with thickness in the range 1.20–4.60 m. Detailed account of uranium mineralization recorded in both the basement granites and cover rock is given below.

In the basement granites, uranium mineralization is hosted essentially by medium- to coarse-grained pinkish-grey granite affected by NW–SE trending fractures. The concentration of radioelements in granite from the non-mineralized areas is much above the normal granite [U: 1.0–93 ppm (avg. 29 ppm), Th: 3–105 ppm (avg. 42 ppm), K: 1.2–8.0% (avg. 4.5%) with U/Th 0.08–3.72 (avg. 1.04); $n = 39$] (Table 1). Granite from mineralized zones usually occurring in the vicinity of fracture zones indicated 0.011–0.077% U_3O_8, (avg. 0.033%) and <0.005–0.016% ThO_2 (avg. 0.009%). U/Th = 0.08–3.32 (avg. 1.04; $n = 15$)) (Table 2). Radiometric surveys in the younger phases of basement granitoids in Nelibanda–Devarabanda area lying to the north of the Kappatralla outlier have also indicated uranium values in the range 0.024–0.170% U_3O_8 with <0.005–0.013% ThO_2. Similarly, granite in the western and southwestern parts of the Kappatralla outlier showed development of secondary uranium minerals such as autunite, with uranium values ranging from 96 to 282 ppm. In the western margin of the Kappatralla outlier, the U/Th ratio (0.22–1.32) indicated an upward enrichment of uranium towards unconformity, thus suggesting the possibility of its upward remobilization from the basement granites. In the central part of the Kappatralla outlier, one borehole intercepted uranium mineralization in fractured granite (0.016% $eU_3O_8 \times 1.0$ m (41.20–42.20 m) and 0.012% $eU_3O_8 \times 1.0$ m (43.40–44.40 m)).

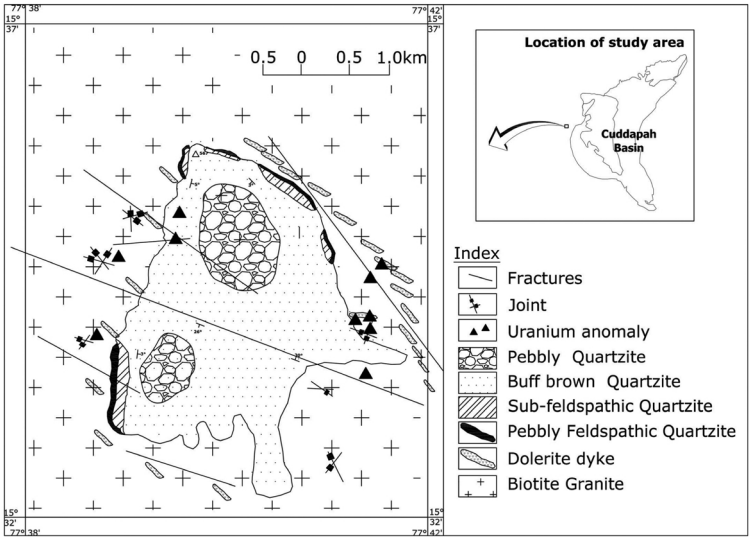

Figure 1. Geological map of Kappatralla outlier, Kurnool district, Andhra Pradesh, India.

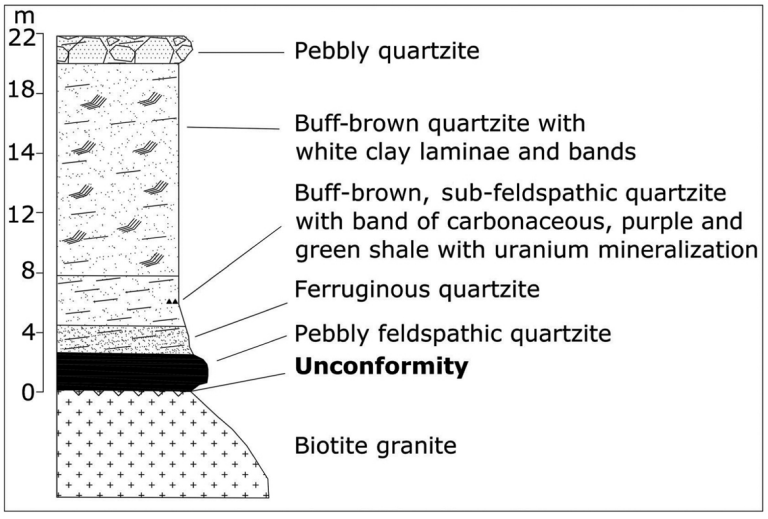

Figure 2. Lithofacies diagram of the Gulcheru Formation in Kappatralla outlier.

Petrographically, basement granites are medium- to coarse-grained with hypidiomorphic granular texture. They are generally fractured and exhibit varying degrees of deformation. Quartz, microcline microperthite, orthoclase–microperthite and plagioclase are the essential minerals whereas biotite, chlorite, sphene, zircon and apatite occur as accessories in decreasing order of abundance. Opaque minerals are rare and represented mainly by pyrite and hydrous iron oxide. At places, microcline microperthite shows post-crystalline deformation with fractures hosting clusters of chlorite, sphene and epidote. Post-deformational hydrothermal alteration is represented by chloritization of biotite and sericitization and illitization of plagioclase.

Gummite (altered uraninite), U–Ti–Fe complex, allanite and zircon are the radioactive minerals in granite. Gummite occurring along fractures records medium density alpha tracks on CN film and is encircled by radial fractures (Figure 3).

Several NW–SE trending fracture zones, prominent in the basement, also cut across the cover sediments of the Gulcheru Formation. Surface uranium occurrences in the area are mostly associated with pebbly sub-feldspathic quartzite member (0.011–0.160% U_3O_8; $n = 14$) (Table 3) proximal to the unconformity,

lying about 3–7 m above it. The uraniferous quartzite is whitish, sub-feldspathic, fractured and has a coating of ferruginous materials. It occurs bounded by two major NW–SE trending faults. Higher grade of uranium mineralization occurs in association with quartzite containing stringers and laminations of carbonaceous shale with pyrite. This feature has also been confirmed by drilling in progress. Surface uranium anomalies located in and around Kappatralla are mainly associated with pebbly feldspathic Gulcheru quartzite (0.011–0.160% U_3O_8; avg. 0.058% U_3O_8) occurring proximal to the unconformity and locally sporadic in fractured basement granites (0.011–0.077% U_3O_8 (avg. 0.033%), <0.005–0.016% ThO_2 (avg. 0.009%)).

Correlatable uranium mineralization has been intercepted in all the seven boreholes drilled, which confirms the subsurface continuity of uranium mineralization in Gulcheru quartzite. Figure 4 presents transverse section along two recently drilled boreholes in the Kappatralla outlier showing correlation of uranium mineralization in Gulcheru quartzite. A mineralized block about 900 m × 400 m in the Kappatralla outlier has been confirmed, and dimension of the mineralized area may increase with drilling in extension areas. Gamma-ray logging of boreholes drilled in the area has indicated the grade of mineralization in the range 0.014–0.190% eU_3O_8 over widths of 1.40–4.60 m at depths ranging from 9.30 to 16.20 m.

Petrographic studies show that uraniferous quartzite is sub-feldspathic, light grey, medium- to fine-grained, moderately sorted, saccharoidal and exhibits moderate maturity. It comprises ~80% (by volume) quartz, which is mainly monocrystalline and commonly exhibits overgrowths (Figure 5). Minor minerals include feldspar, biotite, chlorite and sericite. Chert detritus is also seen. Besides, thin laminations of carbonaceous and greenish shale are conspicuous in the feldspathic quartzite. Various alteration features such as ferrugenization, silicification and kaolinization are common. Textural features indicate that feldspar is less rounded than quartz. Hematite and pyrite are the opaque accessory minerals. Coffinite and pitchblende are the main uranium minerals replacing pyrite (Figure 6). Pyrite appears to be diagenetic in nature, as it forms part of the cement that binds the detrital quartz and feldspar. Coffinite formed from pitchblende due to the addition of silica, and contains relict grains of pitchblende. Coffinite produces medium-density alpha tracks, whereas pitchblende records medium- to high-density alpha tracks on CN films (Figures 7 and 8). Besides, low-order radioactivity in quartzites is also attributed to the presence of zircon.

Granites forming the basement of Gulcheru quartzite in the Kappatralla outlier are fertile as indicated by high uranium with U/Th ratio of 1.04, presence of metamict allanite and labile uranium as evidenced by the presence of secondary uranium minerals. Low-density alpha tracks from the xenomorphic materials of radial fractures around biotite, allanite and hydrated iron oxides indicate the presence of labile uranium in the system[6]. Further, mobilization of parent uranium from mineralized granite along fracture zones is indicated by radioactive disequilibrium in favour of daughter elements of uranium[7] (avg. 0.51, $n = 15$). Radial fractures around metamict minerals suggest expansion in the volume of radioactive minerals due to metamictization. Metamict minerals expel brown-coloured xenomorphic materials, occupying the radial fractures in host minerals. Mineralization in granite is accompanied by sericitization and illitization of plagioclase,

Table 1. Radio elemental abundance in non-mineralized granite ($n = 39$)

	U (ppm)	Th (ppm)	% K	U/Th	KxU/Th
Average	29	42	4.59	1.04	5.85
Range	1–93	3–105	1.20–8.00	0.08–3.32	0.30–12.98

Table 2. Radiometric assay of mineralized granite ($n = 15$)

	% eU_3O_8	% U_3O_8	% ThO_2	% Ra (eU_3O_8)	U_3O_8/ThO_2
Average	0.028	0.033	0.009	0.028	1.04
Range	0.014–0.056	0.011–0.077	<0.005–0.016	0.011–0.051	0.08–3.32

Table 3. Radiometric assay of mineralized sub-feldspathic quartzite ($n = 14$)

	% eU_3O_8	% U_3O_8	% ThO_2	% Ra (eU_3O_8)	U_3O_8/Ra (eU_3O_8)
Average	0.049	0.058	<0.005	0.049	1.16
Range	0.011–0.12	0.011–0.160	<0.005	0.011–0.120	0.72–1.51

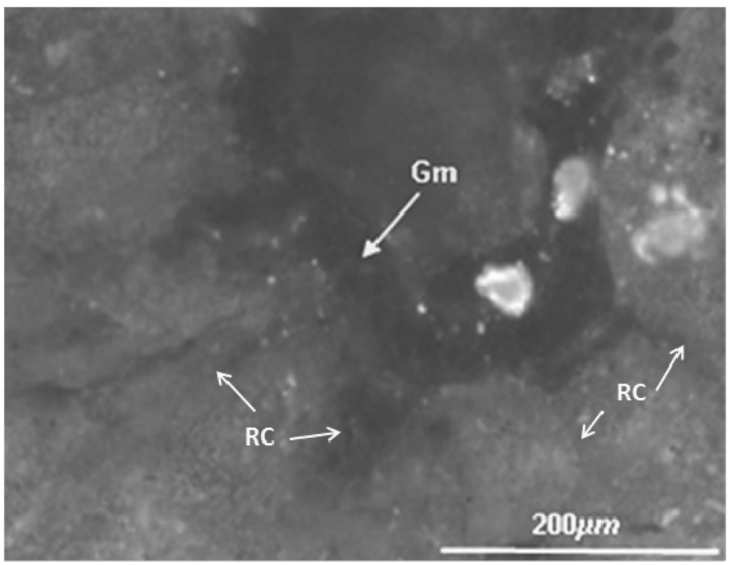

Figure 3. Gummite (Gm) around metamict mineral and brownish-coloured radioactive materials in radial cracks (RC). TL, 1N.

chloritization of biotite and hematitization, representing hydrothermal alteration.

Repetition of pebble beds in Gulcheru quartzite indicates cyclic sedimentation[8]. Pebbly bed of topmost unit of the Gulcheru Formation is enriched in quartz pebbles compared to the pebbly bed exposed close to unconformity, suggesting an increase in the maturity of sediments in the distal part[9]. Moderate mineralogical maturity of sediments is indicated by the presence of unstable minerals like microcline, and kaolinized and sericitized grains of feldspar along with quartz[10]. Silica overgrowths around quartz suggest reduction of porosity of rocks during diagenetic changes[11]. Thin laminations of carbonaceous shale in feldspathic quartzite indicate prevalence of reducing depositional environment[12].

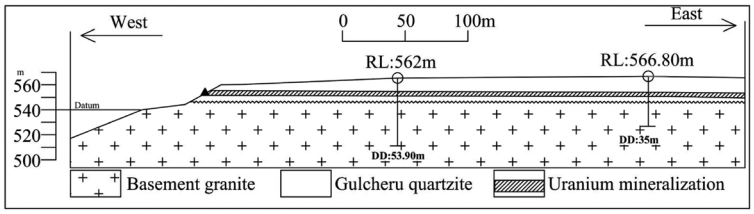

Figure 4. Section along two boreholes in Kappatralla outlier showing correlation of uranium mineralization in Gulcheru quartzite.

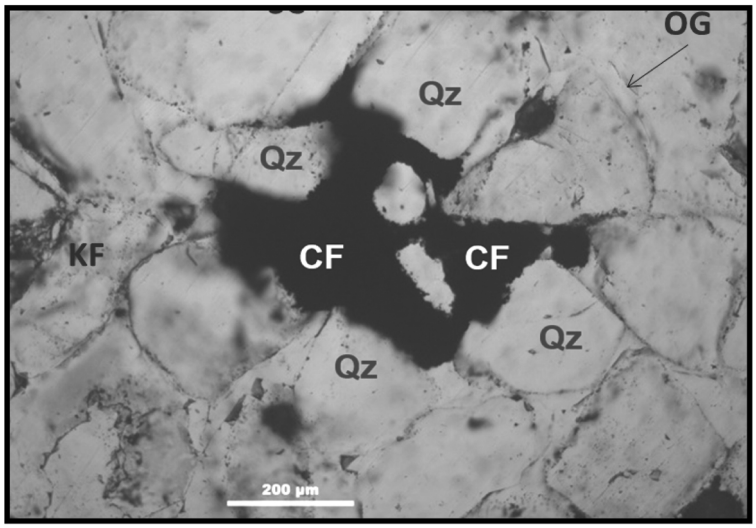

Figure 5. Overgrowth around quartz in feldspathic quartzite and precipitation of coffinite (CF) around grain boundaries of quartz (Qz). TL, 1N.

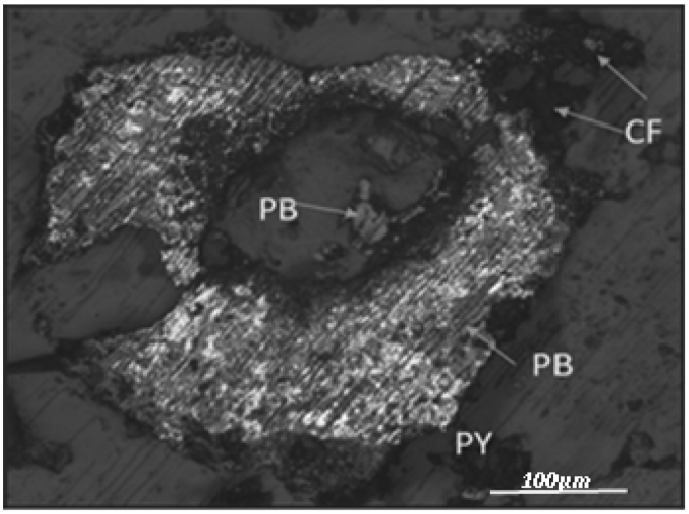

Figure 6. Replacement of pyrite (PY), by pitchblende (PB) and formation of coffinite (CF) from pitchblende (PB). RL, 1N.

High value of U_3O_8/Ra (eU_3O_8) in quartzite (0.722–1.50, avg. 1.15; $n = 14$) indicates dominance of parent radionuclides in mineralized quartzite, which might have got mobilized from the granite during reactivation. This is evident from the observation that granites of the fracture zone are depleted in the parent. Pitchblende and coffinite in quartzite are epigenetic in nature and occur as fine veins, fracture/cavity fillings and around grain boundaries. Other ore minerals include pyrite, chalcopyrite and pyrrhotite. It is observed that carbonaceous shale and pyrite normally occur in mineralized horizons, which suggests prevalence of reducing environment causing fixation of uranium from the mineralized solution[12].

Based on these observations, the unconformity contact zone and overlying sediments are being actively explored for unconformity-related uranium mineralization. It is surmised that mineralization along the unconformity plane between granitoids and overlying sediments and also within overlying cover sediments (Gulcheru quartzite) could be of higher grade as the sediments provide a secure cover focusing the mineralizing solutions. The uranium mineralization could be concentrated in the sediments affected by NW–SE trending fractures prevalent in the area.

The potentiality of the Kappatralla outlier is substantiated by the boreholes, which intercepted significant correlatable bands with grade 0.014–0.190% eU_3O_8 and widths 1.40–4.60 m at depths ranging from 9.30 to 16.20 m over 900 m × 400 m block, confirming the subsurface continuity of uranium mineralization in Gulcheru quartzite.

Based on the integration of geological, structural and radiometric survey data, it is concluded that the NW–SE trending fracture zones within the younger granites and cover sediments are favourable to host better-grade uranium mineralization. Tabular nature of ore body in porous feldspathic quartzite containing

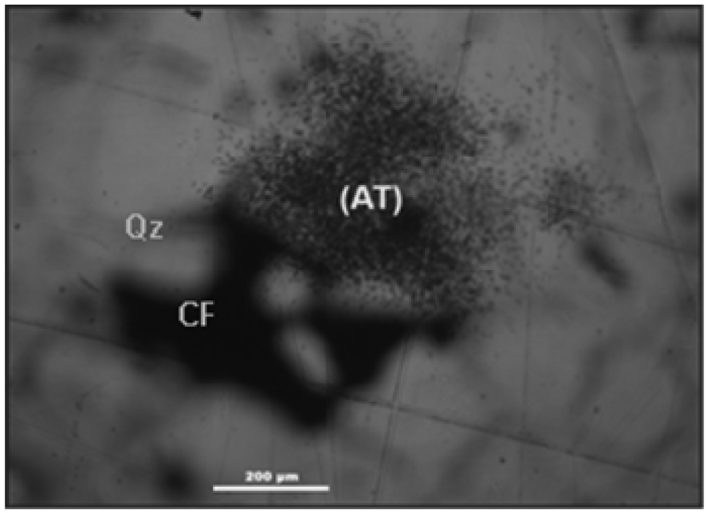

Figure 7. Alpha tracks (AT) due to coffinite (CF) precipitated around quartz (Qz). TL, 1N.

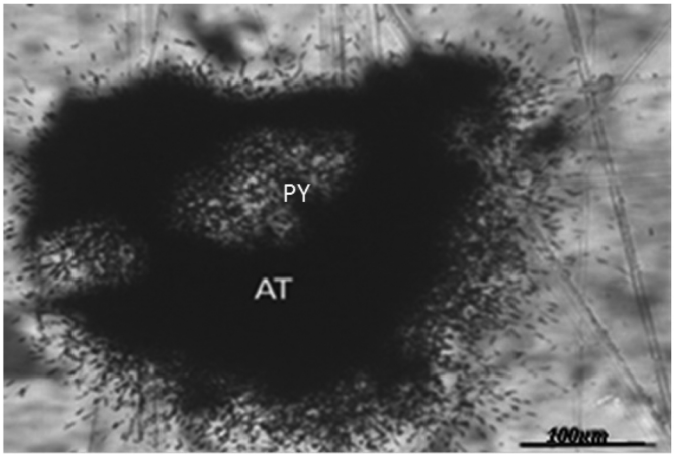

Figure 8. Alpha tracks (AT) due to pitchblende (PB) precipitated at the expanse of pyrite (PY). RL, 1N.

carbonaceous matter, and spatial and temporal relation to the fracture zones suggest epigenetic nature for uranium mineralization in the Kappatralla outlier. Post-sedimentary fracturing events might have rendered secondary porosity, thereby producing locales conducive for migration and localization of mineralizing solutions within the sediments. The mineralizers precipitated uranium in reducing environments favoured by carbonaceous shale and pyrite. Besides, the clay formed out of feldspar in the quartzite also adsorbed uranium. Continued hydrothermal activity in areas bound by NW–SE trending fracture zones might have played a major role in enrichment and improvement of grade of uranium mineralization.

1. King, W., *Mem. Geol. Surv. India*, 1872, **8**, 346.
2. Nagaraja Rao, B. K., Rajurkar, S. T., Ramalinga Swamy, G. and Ravindar Babu, B., *Mem. Geol. Soc. India*, 1987, **6**, 33–86.
3. Umamaheswar, K., Basu, H., Patnaik, J. K., Ali, M. A. and Banerjee, D. C., *J. Geol. Soc. India*, 2001, **57**, 405–409.
4. Dwivedi, A. K., Hegde, G. N. and Umamaheswar, K., *J. Geol. Soc. India*, 2006, **67**, 197–200.
5. Bhopal Reddy, A. and Rao, K. S., District Resource Map of Kurnool district, AP, Geological Survey of India, 1999,
6. Darnley, A. G., In *Uranium in Granites*, (ed. Maurice, Y. T.), Geological Survey of Canada, 1982, Paper 81-23, pp. 1–10.
7. Steenfelt, A., *Mineral. Mag.*, 1982, **46**, 149–161.
8. William, P. F. and Rust, B. R., *J. Sediment. Petrol.*, 1969, **39**, 649–679.
9. Reineck, H. E. and Singh, I. B., *Depositional Sedimentary Environments*, Springer-Verlag, 1973, p. 439, ISBN 3-540-06115-0.
10. Dickinson, W. R. *et al.*, *Geol. Soc. Am. Bull.*, 1983, **64**, 233–235.
11. Leder, F. and Park, W. C., *Am. Assoc. Petrol. Geol. Bull.*, 1986, **70**, 1713–1728.
12. Breger, I. A. and Deul, M., International Conference on Peaceful Uses of Atomic Energy (Proceedings of Conference Geneva, 1955–56), UN, New York, USA, 1956, p. 418.

ACKNOWLEDGEMENT. We thank our colleagues in the Petrology and Physics Groups, Atomic Minerals Directorate for Exploration and Research, Department of Atomic Energy, Hyderabad for their valuable contribution.

Received 18 November 2018; revised accepted 13 February 2019

H. S. RAJARAMAN*,†
S. K. JAIN
B. S. BISHT
A. V. JEYAGOPAL†
M. B. VERMA

Atomic Minerals Directorate for Exploration and Research, Department of Atomic Energy, Hyderabad 500 016, India
**For correspondence.*
e-mail: hsr.amd@gmail.com
†Equally contributed.